OXFORD

SOT | Society of Toxicology
www.toxsci.oxfordjournals.org

TOXICOLOGICAL SCIENCES, 148(2), 2015, 421–432

doi: 10.1093/toxsci/kfv194
Advance Access Publication Date: October 5, 2015
Research Article

N-(2-Aminoethyl) Ethanolamine-Induced Morphological, Biochemical, and Biophysical Alterations in Vascular Matrix Associated With Dissecting Aortic Aneurysm

Zhenping Chen,* Ya Xu,* Paul Bujalowski,† Andres F. Oberhauser,†,‡ and Paul J. Boor*,[1]

*Department of Pathology; †Department of Neuroscience and Cell Biology; and ‡Sealy Center for Structural Biology and Molecular Biophysics, University of Texas Medical Branch, Galveston, Texas 77555

[1]To whom correspondence should be addressed Paul J. Boor, Department of Pathology, University of Texas Medical Branch. 301 University Blvd, Galveston, Texas 77555. Fax: (409) 747-1763. E-mail: pboor@utmb.edu

ABSTRACT

Dissecting aortic aneurysm (DAA) is an extended tear in the wall of the aorta along the plane of the vascular media. Our previous studies indicated in a developmental animal model, that DAA was related to pathological alteration in collagen, especially collagen type III. Accordingly, in the present studies, neonatal aortic vascular smooth muscle cells (VSMC) and timed pregnant Sprague-Dawley rat dams were treated with *N*-(2-aminoethyl) ethanolamine (AEEA), which, as shown previously, causes DAA in offspring. Morphological changes in extracellular matrix (ECM) produced by VSMC *in vitro* were detailed with scanning electron microscopy (SEM), and biochemical changes in cells and ECM produced by VSMCs were defined by Western blotting. Biophysical changes of the collagen extracted from both the ECM produced by VSMC and extracted from fetal rat aortas were studied with atomic force microscopy (AFM). ECM disruption and irregularities were observed in VSMCs treated with AEEA by SEM. Western blotting showed that collagen type I was much more extractable, accompanied by a decrease of the pellet size after urea buffer extraction in the AEEA-treated VSMC when compared with the control. AFM found that collagen samples extracted from the fetal rat aortas of the AEEA-treated dam, and in the *in vitro* formed ECM prepared by decellularization, became stiffer, or more brittle, indicating that the 3D organization associated with elasticity was altered by AEEA exposure. Our results show that AEEA causes significant morphological, biochemical, and biomechanical alterations in the ECM. These *in vitro* and *in vivo* strategies are advantageous in elucidating the underlying mechanisms of DAA.

Key words: dissecting aortic aneurysm (DAA); aorta; vascular smooth muscle cells (VSMCs); vascular extracellular matrix (ECM); *N*-(2-aminoethyl) ethanolamine (AEEA); collagen

The human vascular disorder known as dissecting aneurysm is a potentially life-threatening condition in which a tear or rent in a blood vessel "dissects" along the plane of the vascular media. Although it may occur in any large or medium-sized artery, dissection most commonly involves the thoracic aorta, where it is known as dissecting aortic aneurysm (DAA). The tear or rent of DAA may extend down the aorta and into nearby anatomic structures or spaces and, thus, result in sudden death (Criado, 2011; Goldfinger *et al.*, 2014; Pannu *et al.*, 2005). DAA affects persons of any age past puberty, and is thought to be the most common cause of death related to the human aorta (Elefteriades, 2008).

Our laboratory recently established an animal model of aortic dissection in order to facilitate the study of DAA. This

chemical-induced model of aortic dissection morphologically mimics DAA in the human, and thus may serve as an excellent testing ground to uncover changes that underlie vascular dissection (Boor *et al.*, 2006; Gong *et al.*, 2006; Xu *et al.*, 2014). In this model, pregnant rat dams are exposed during the last trimester of pregnancy to semicarbazide (Gong *et al.*, 2006) or the industrial chemical *N*-(2-aminoethyl) ethanolamine (AEEA) (Xu *et al.*, 2014). Rat pups born to treated dams develop an extensive DAA in a dose-dependent fashion, at the time of birth, when blood pressure rises. Hence, the fetus examined just prior to birth does not exhibit the DAA, allowing study of the uninterrupted aortic wall on GD21, this developmental DAA occurs with no overt generalized toxicity to dam, fetuses, or newborn rat pups (Gong *et al.*, 2006; Xu *et al.*, 2014). The DAA phenomenon induced by AEEA was first described by workers at the Laboratory of Reproduction Toxicology and Pathology of BASF Ludwigshafen, Germany (Moore *et al.*, 2012) and bears remarkable morphologic similarity to human DAA. The aliphatic amine AEEA, which is produced by BASF and DOW, has widespread industrial use in the production of fabric softeners, chelating agents, hardeners, and soldering fluxes (Moore *et al.*, 2012). Exposures to humans have also been shown to occur in cable joiners in the electronics industry who used AEEA containing soldering fluxes (Goh, 1985; Pepys and Pickering, 1972; Sterling, 1967), and through contamination of residential water wells. A major intermediate in a host of industrial syntheses, AEEA, has been found in a variety of household products, and as a trace contaminant of women's cosmetics (Foti *et al.*, 2001).

Findings in our previous animal studies in rat established a clear dose-response relationship, and implicated aberration in collagen development (especially in collagen type I and III) in the etiology of DAA (Xu *et al.*, 2014). These collagens are the major extracellular matrix (ECM) components in developing aorta (Arteaga-Solis *et al.*, 2000). Type III collagen, specifically, is thought to be essential for the regulation of the vascular type I collagen fibrillogenesis. Our previous study (Gong *et al.*, 2008) suggested that collagen type III, as the precursor collagen thought to be important in ECM development, is the primary target of AEEA's *in utero* effect. Changes in elastin, or in other connective tissue elements, such as the fibrillins, were not found in those *in vivo* studies.

While this chemical-induced animal model of aortic dissection provides a useful testing ground for studying the mechanisms that underlie vascular dissection, *in vitro* models, on the other hand, may offer many advantages. However, literature using *in vitro* ECM to study DAA and other vascular phenomenon is scanty. In the present studies, therefore, we first evaluated the morphological and biochemical changes in cells and ECM produced by neonatal aortic vascular smooth muscle cells (VSMC) exposed to AEEA. Neonatal VSMCs generate abundant ECM by 10 days post-seeding (Langford *et al.*, 2002). We show in the present studies that AEEA-exposure to VSMCs results in striking ECM morphological defects when examined under scanning electron microscopy (SEM). Western blotting showed that collagen type I was much more extractable, accompanied by a decrease in the sample pellet sizes after urea buffer extraction. In order to further characterize and compare the effects of AEEA on the structure of the extracted aortic collagen and ECM samples, we used atomic force microscopy (AFM) techniques. The main advantage of AFM is that it allows nano-scale mechanical measurements on native samples, and thus can help elucidate the effects of AEEA on the physical properties of the vascular ECM. AFM examination showed that both the collagen samples extracted from the fetal rat aortas of the AEEA treated dam, and the *in vitro* formed ECMs prepared by decellularization, became stiffer, suggesting that their 3D organization associated with elasticity was altered. These data further define ECM defects in this experimental model of DAA and show that the *in vitro* strategies may be employed in elucidating the mechanisms of arterial dissection.

MATERIALS AND METHODS

Materials. AEEA was supplied by BASF SE, GV/T-Z470, 67056 Ludwigshafen, Germany (Lot number: AE4A0790H0; purity 99.8%). RIPA buffer (Radioimmunoprecipitation assay buffer) (Alcaraz *et al.*, 1990; Ngoka, 2008) contains 25 mM Tris-HCl pH 7.6, 150 mM NaCl, 1% NP-40, 1% sodium deoxycholate, and 0.1% SDS. Urea extraction buffer was modified based on the "4 × LOX-buffer" (Bertram and Hass, 2009), which contains 4.8 M urea, 200 mM sodium phosphate buffer, pH 7.4. Trizma base (T-8524), sodium deoxycholate (D6750), sodium phosphate dibasic (S0876), sodium phosphate mono basic (S0751), urea (U5128), MTT (M2128), Tween 20 (P9416), and albumin bovine serum (BSA, A9647) were purchased from Sigma. Sodium chloride (Catalog # 7581) was from Mallinckrodt. NP-40 was from Fluka (Catalog # 74385). SDS was from Bio-Rad (Catalog # 1610301). Halt phosphate inhibitor cocktail was purchased from Thermo Scientific (Catalog # 78420). Protease inhibitor cocktail (cOmplete, EDTA-free Protease Inhibitor Cocktail Tablets) was ordered from Roche Diagnostics (Catalog # 05056489001). Novex NuPAGE SDS-PAGE gels (4-12% Bis-Tris Pre-Cast gels, NP0321) were obtained from Invitrogen. PVDF membrane was the product of BioRad. Antibodies against collagen I (ab34710), collagen III (ab6310), α-smooth muscle actin (α-SMA) (ab5694) and secondary antibodies including anti-rabbit and anti-mouse IgG antibodies conjugated to horseradish peroxidase (ab6721 and ab6728, respectively) were ordered from Abcam. CL-XPousure films were from Thermo Scientific; and ECL Western blot detection reagents were from Amersham Biosciences (RPN2209).

Animal treatment. Timed pregnant Sprague-Dawley rat dams, 250-300 g (obtained from Harlan Laboratories, Inc), were treated with AEEA (50 mg/kg, $n = 8$) by gavage on 14 days gestation. In our previous studies, at that dosage, the incidence of DAAs diagnosed on both gross and microscopic grounds was 21/24 (88%) in pups (Xu *et al.*, 2014). Rat dams were treated with normal saline (NS) as control ($n = 5$ in gavage group). All treatments were administered daily at approximately the same time of day, on gestation days 14–20; this gestational period in rodents was chosen because this is when active development and differentiation of the vascular wall, or media of large elastic and medium-sized arteries occurs (Gong *et al.*, 2008; Nakamura, 1988). All animal usage was performed under protocol #8812178 approved by the Institutional Animal Care and Use Committee at the University of Texas Medical Branch.

Preparation of collagen from aortas of fetal rats. Rat fetuses from dams treated with either AEEA or NS in controls were killed on gestational day 20 (estimated day before birth) as described above. The entire thoracic aorta was carefully removed *en bloc*. Specimens were dissected fresh. Anatomic dissection of isolate aortas was done under an Olympus SZ61 Zoom Stereo dissecting microscope. Total aortic collagen was extracted in 178 fetuses (pooled into 4 groups from 13 pregnant rats) harvested from pregnant rats treated either with 50 mg/kg AEEA or PBS daily. Pooled aortas (107) from fetuses from 8 AEEA-treated pregnant rats were divided into 2 groups, and 71 aortas pooled

from fetuses from 5 control (PBS-treated) pregnant rats were divided into 2 groups for studies, respectively, according to our published methods (Gong *et al.*, 2006), which was modified based on techniques of Chandrakasan *et al.* (1976). The aortas were dissected free of extraneous tissue, rinsed with PBS, blotted dry, weighed, minced, and extracted with a 3:1 volume ratio mixture of ethanol-ether at 4°C for 30 min for defatting. The samples were then dried under nitrogen and followed by vacuum-desiccation. Dry fat-free weights were determined. Tissues were extracted multiple times with 0.5 M NaCl for 48 h at 4°C, and then with 0.5 M acetic acid for another 48 h at 4°C. The supernatants of the acetic acid extracts, which contain collagen, were dialyzed for 24 h against deionized water, frozen in 1.5-ml tubes, speed-vac dried, and weighed. The collagen samples were then suspended in deionized H_2O and heated at 98°C for 5 min to prepare 2.5% collagen solution, which was transferred to a 13-mm diameter round coverslip, cooled, and then dried in a refrigerator at 4°C overnight, followed by vacuum-desiccation, before AFM studies.

Neonatal rat aortic smooth muscle cell (VSMC) culture. Litters of 8-12 Sprague-Dawley neonatal rat pups were used for establishing cell lines. Thoracic aortas from the pups were harvested within 24-36 h after normal vaginal birth. Aortas were minced, and VSMC were dissociated in a collagenase-trypsin solution (10 mg collagenase and 50 mg trypsin in 20 ml PBS). VSMCs were collected by low-speed centrifugation and plated in 75 cm^2 flasks that had a medium containing Dulbecco's (low-glucose) modified Eagle medium, 10% fetal calf serum, and 100 U of penicillin-100 μg streptomycin/ml. Positive Western blot detection with α-SMA characterized cell lines as VSMCs. These cells were used during serial passages 3-8. Cells maintained in culture for weeks exhibited VSMC growth characteristics, including forming copious amounts of matrix material visible to the unaided eye and growing into hill-and-valley microscopic patterns (Langford *et al.*, 2002) as well as embedding themselves in the surrounding matrix.

Cytotoxicity assay of AEEA to VSMCS. The cytotoxicity of AEEA toward VSMCs was measured using the MTT cytotoxicity assay as previously modified (He *et al.*, 1998; Yang *et al.*, 2004). In brief, 5000-10 000 cells in 100 μl aliquots of growth medium were plated into 96-well cell culture plates, incubated at 37°C for 48 h. Four hours prior to treatment, the medium was removed and replaced with fresh medium. Cells were exposed to various concentration of AEEA for a total of 24 h. Five replicate wells were used for each assay in 3 separate experiments. At 20 h post-treatment, MTT was added to each well at a final concentration of 0.5 mg/ml. The plates were incubated for another 4 h at 37°C, followed by removal of the medium and addition of 10 μl of DMSO and 90 μl of isopropanol at room temperature to solubilize the formazan crystals. Absorbance was read at 570 nm with a microplate reader (Bio-Rad 3550-UV Plate Reader; Hercules, California). Absorbance values were normalized to control wells and expressed as a percentage of the control. The lethal concentration producing 50% reduction in MTT absorbance (LC50) was determined for each plate by interpolation.

Preparation of decellularized matrix produced by aortic VSMCS. Cultured neonatal rat aortic smooth muscle cells are capable of accumulating collagen and elastin in their ECM beginning at day 6 or 7, to large amounts at 10 days after seeding. This affords a useful sample of matrix for examining changes in the ECM *in vitro*, though the elastin content is drastically reduced when the cells are derived from the aortas of older animals, which is why the neonatal cells were used in the present experiments (Davidson *et al.*, 1997; Langford *et al.*, 2002; Oakes *et al.*, 1982).

VSMCs were cultured on 13 mm diameter Nunc Thermanox Coverslips (Catalog #174950) in 24-well cell culture plates in DMEM supplemented with 10% FCS, antibiotics, and 50 μg/ml of sodium ascorbate, with the intention that cell density reaches 70% confluence the next day. AEEA treatments (0.00, 0.05, 0.25, and 0.50 mM) were started before the formation of ECM, usually at the second day post-passage. Sodium ascorbate, which is the crucial cofactor of lysyl oxidase (LOX), lysyl hydroxylase, and proline hydroxylase, was added every day, 5 days/week, to stimulate ECM assembly (Davidson *et al.*, 1997). AEEA was changed whenever culture media were changed (every 3 days). After 14 days of culture, the resulting tissue sheets were gently rinsed twice with PBS, and then incubated in sterile deionized water for 20 min at 4°C to lyse the cells at hypotonic condition for decellularization. The water was then changed, and ECM samples were kept overnight at 4°C. The next day, the water was replaced with PBS (Bourget *et al.*, 2012). The ECM samples were either to be for AFM coverslips, or fixed for SEM. For fixation of ECM samples for SEM, slides were washed twice with PBS, and samples were immersed in Karnovsky's fixative (Graham and Karnovsky, 1966) at room temperature for 30 min. Karnovsky's fixative contains 2% paraformaldehyde; 2.5% glutaraldehyde in 0.1 M phosphate buffer pH 7.4. The ratio of fixative volume to specimen size was ~20:1. After fixation, the fixative was aspirated and specimens were washed twice for 2 min in 3 ml 0.1 M phosphate to remove excess fixative, and then they were dehydrated in ×20 volume of 30% ethanol for 10 min on a shaker. Samples were then dehydrated through successive ethanol at 50, 75, 95, and 100%, each for 10 min. Samples were placed in 50% *tert*-butanol in ethanol for 10 min, and then dried and coated and scanned using a conventional scanning electron microscope.

Western blots. Cultured VSMCs grown and treated with AEEA as described above were gently washed with 4°C pre-chilled PBS. The plate was then placed on the surface of a −20°C ice block immediately. RIPA buffer was added to the cells, which were then gently scraped off and transferred to pre-ice chilled centrifuge tubes. The cells were suspended by pipetting up and down and then the samples were incubated on ice for 15 min. Extracts were spun at 14 000 rpm at 4°C for 15 min with a bench centrifuge, and supernatants were saved. For the second extraction, pellets were then back-extracted by resuspending in urea lysis buffer, brief sonication, incubation on ice for 15 min, and centrifugation as above, saving supernatants. The protein concentrations of the samples extracted with RIPA were measured by with the DC protein assay kit (Bio-Rad Laboratories, Inc, Hercules, California), whereas the protein of urea extracts was quantitated with the BCA protein assay (Pierce). 20 μg proteins for each sample were subjected to standard SDS-PAGE. The separated proteins were transferred to PVDF membrane (BioRad) and blocked with 3% BSA (Sigma) in TBS-T, and then probed with the appropriate antibodies. Signals were recorded on film by using ECL Western blot detection reagents.

Atomic force microscopy. The mechanical properties of aorta collagen samples and deposited extracellular matrices were studied using a self-built single molecule AFM (Bullard *et al.*, 2002; Miller *et al.*, 2006; Oberhauser *et al.*, 1998; Rabbi and Marszalek, 2007) that consists of a detector head (Digital Instruments) mounted on top of a single axis piezoelectric positioner with a strain

gauge sensor (P841.10, Physik Instrumente). The P841 has a total travel of 15 μm and is attached to 2 piezo-electric positioners (P280.10A, Physik Instrumente) that are used to control the x and y positions. This system has a z-axis resolution of a few nanometers and can measure forces in the range of 10–10 000 piconewtons (pN). The monitoring of the force reported by the cantilever and the control of the movement of the piezoelectric positioners are achieved by means of 2 data acquisition boards (PCI 6052E, PCI 6703, National Instruments) and controlled by custom-written software (LabView; National Instruments and Igor, Wavemetrics).

For AFM compression experiments we used sharp pyramidal tips (radius ~20 nm; MLCT, Veeco Metrology Group, Santa Barbara, California). The spring constant of each individual cantilever was calculated using the equipartition theorem (Florin *et al.*, 1995). The rms force noise (1-kHz bandwidth) was ~10 pN. Unless noted, the compression and pulling speed of the different force-distance curves was in the range of 0.1-0.5 nm/ms.

Estimation of the young modulus using AFM. With the AFM, a controlled deformation was applied to the sample and the compressive forces were measured through the cantilever deflection (Fig. 4A). The force-displacement (F-x) curves were produced by converting cantilever deflection (d) into force (F) by means of $F = kd$, where k is the cantilever spring constant. The Young modulus (E) was estimated by fitting the compression force-displacement curves to a standard Hertz model for a parabolic tip (Achterberg *et al.*, 2014; Engler *et al.*, 2007; Frey *et al.*, 2007; Lin *et al.*, 2007; Loparic *et al.*, 2010; Stolz *et al.*, 2004):

$$F_{tip} = \frac{4}{3\pi}\frac{E}{1-\nu^2}\sqrt{R_{tip}} \times \delta^{\frac{3}{2}}, \quad (1)$$

where $\nu = 0.5$ is the Poisson ratio, R_{tip} is the tip radius, and δ is the indentation depth, calculated by subtracting the cantilever deflection from the tip displacement. To obtain accurate elasticity measurements every sample a region of 100×100 nm^2 was probed by running 100 force-displacement curves. The contact stiffness has the dimension of force per unit length and is calculated as the derivative of the upper ~30% of the unloading part of the compression curve.

As a reference we use agarose gel films since their Young modulus is well known (Loparic *et al.*, 2010; Stolz *et al.*, 2004); the films were prepared using 2.5% (w/w) agarose (Sigma) in water as previously described (Stolz *et al.*, 2004).

RESULTS

Impairment of ECM Prepared From the AEEA-Treated Cells

To further explore the mechanisms involving the formations of DAA, in separate experiments, the VSMCs were treated with AEEA (0.00, 0.05, 0.25, and 0.50 mM) for 14 days, and then the decellularized matrix scaffolds were prepared as described above. Observed under optical microscope just before performing decellularization, cells treated with varying concentration of AEEA looked viable. Only rare dead cells were seen. ECM was then prepared and SEM performed. At the low power (×6000 magnification), the decellularized matrix scaffolds prepared from the control cells were integrated and relatively flat. However, in samples in which VSMCs were exposed to AEEA, pits and irregularities in the decellularized matrix scaffolds were observed; the size and occurrence of the pits appeared to increase with increasing AEEA concentration (Fig. 1A). When observed at high power (×20 000 magnification), the decellularized matrix scaffolds prepared from the control cells were integrated and relatively flat, whereas in decellularized matrix scaffolds prepared from the AEEA-treated (0.50 mM) cells, pits, and holes, with diameter up to 2 μm, were observed (Fig. 1B). These data indicate that AEEA markedly alters the production of the ECM *in vitro*.

Measurement of AEEA Cytotoxicity

The cytotoxic effects of AEEA to primary cultured smooth muscle cells were evaluated with the standard MTT assay to determine the cell viability as described above. Cells were exposed to various concentrations of AEEA (0.0, 5.0, 10.0, 15.0, 17.5, 20.0, and 25.0 mM) for 24 h. The cytotoxic AEEA concentration affecting viability in primary cultured aortic smooth muscle cells was ~18 mM (Fig. 2).

Analysis of Collagen Type I and III Proteins From in vitro Samples by Western Blotting

To further understand the biochemical mechanisms of the biophysical and micro-morphological aberrations in vascular matrix, we examined collagen type I and III with Western blotting. Neonatal VSMCs were treated with varying concentrations of AEEA (0.00, 0.10, 0.25, 0.50, 1.00, 2.50, and 5.00 mM) for 10 days. Although cross-linked collagens are not soluble, the non-cross-linked collagens are extractable, depending on the strength of the extracting solution. Therefore, the samples were serially extracted with RIPA buffer and-then urea extraction buffer, as described above. The proteins were then examined with antibodies against collagen type I and III, as well as α-SMA. Our results show that collagen type I was much more extractable or soluble in RIPA buffer. The intensities of the bands corresponding to collagen type I increased accordingly in a dose-dependent manner, except in samples treated with 1.0 mM AEEA, in which band intensity also increased, but not as substantially as that seen in cells treated with 0.50 or 2.50 mM AEEA. An increase was detected in the samples from the cells treated with the lowest concentration tested 0.10 mM AEEA. The band intensity appeared to peak at 2.50 mM (Fig. 3A, left panel).

In the urea extractions (which contain the proteins not soluble in the earlier RIPA extractions) the collagen type I band intensities again increased in the AEEA-treated samples in a dose-dependent manner, which appeared to peak at the 0.5 mM AEEA concentration. Urea buffer extracted more collagen type I than that of RIPA buffer, though it was the second extraction, in which the RIPA soluble collagen type I was already extracted, and accordingly only the RIPA insoluble fraction remained. The blots were re-probed with α-SMA to confirm that the cells were vascular VSMCs. The band intensities of α-SMA were identical, which also shows that the amounts of each sample loaded were equal. Blots of RIPA fractions were re-probed with GAPDH as on additional loading control, and band intensities were similar (Fig. 3A, left panel). Since most of GAPDH proteins were extractable in RIPA buffer, little GAPDH remained in each pellet. Accordingly, the intensities of GAPDH bands in urea were very weak (data not shown). We also examined collagen type III which was barely detected in most of our *in vitro* experiments (data not shown).

We then did time course studies. VSMCs were treated with 0.50 mM AEEA, as that was the relative lowest concentration capable of causing significant increase of extractable collagen type I. Cells were harvested at 4, 7, 10, and 14 days post-AEEA treatment. The results clearly showed that in the RIPA fraction, the amounts of extractable collagen type I increased at all the time points tested, and peaked at 7 days. Again, similar to that

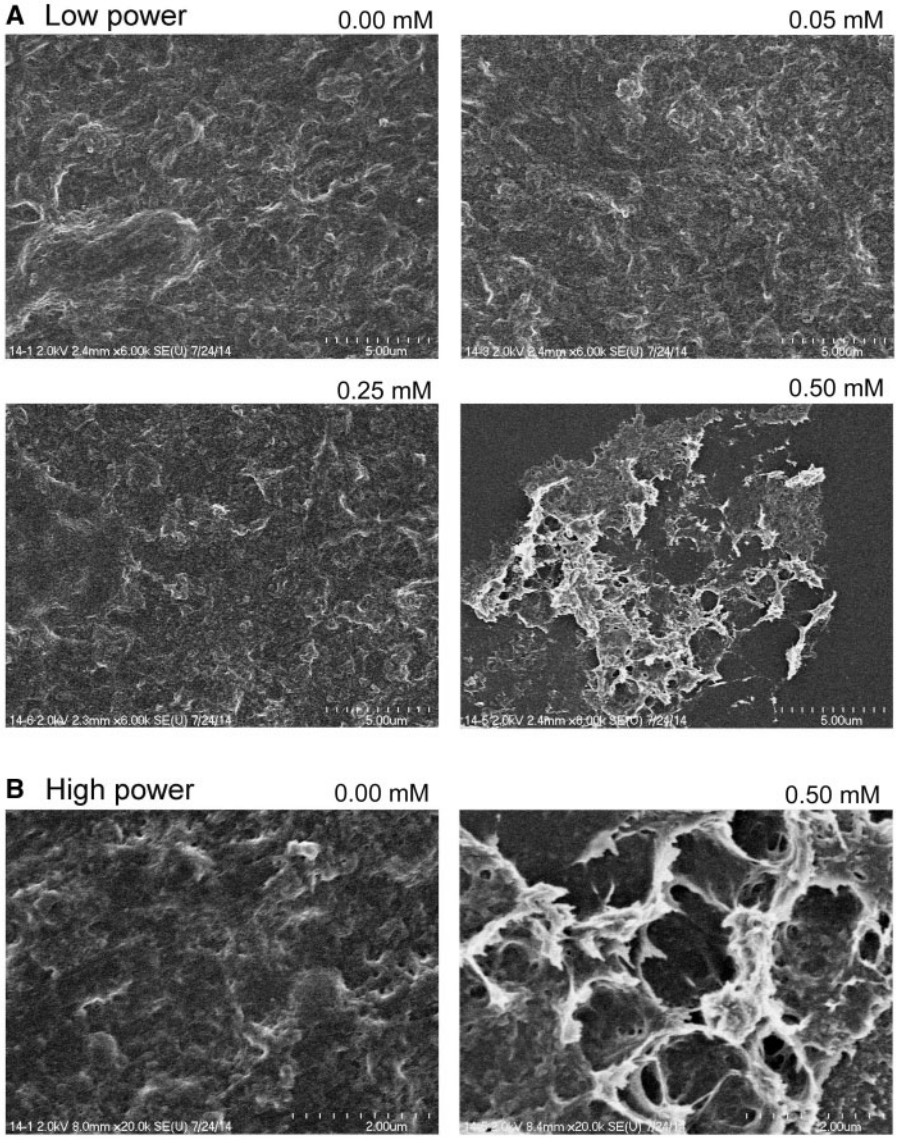

FIG. 1. SEM: ECM prepared from the cells treated with AEEA (0.00, 0.05, 0.25, or 0.50 mM) for 14 days. **A**, Low power (×6000 magnification). **B**, High power (×20 000 magnification).

in the dose-response experiments, most of the collagen type I was in the urea fraction; re-probing with α-SMA and GAPDH showed the characteristic-SMA and equal loading. Changes of collagen type III were also investigated in the time course. In the RIPA fraction, collagen III appeared to drop at earlier time (4 days) point, and then no significant change was detected, while the intensity of the control bands decreased. In the urea fraction, collagen type III was decreased slightly (Fig. 3B).

Consistent with the collagens being much more extractable in the AEEA-treated samples, particularly in urea buffer, the visible sizes of the pellets also were smaller after urea extraction but appeared only slightly decreased after RIPA extraction as well (data not shown). In addition, the urea extracted pellets appeared to have a less dense appearance. These findings indicate a profound effect on collagen metabolism and overall production; we are tentatively concluding that this effect is due to perturbations of the normal cross-linking within the collagen molecule that is primarily responsible for its structural strength.

Mechanical Properties of Aorta Collagen Samples Extracted From AEEA-Treated Fetuses by Nano-Indentation

In order to further quantify and better understand the effects of AEEA on the structure of the extracted aorta collagen and ECM samples, we used AFM nano-indentation techniques (Fig. 4A). As reference points we used agarose and mica. Agarose serves as a reference for tissue-like material, since its elastic modulus has been characterized with AFM (the elastic modulus of 2.5% agarose is ~25 kPa) and has mechanically isotropic structure at the nano- and micrometer scale (Loparic *et al.*, 2010; Stolz *et al.*, 2004). Mica is a very stiff material with simple structural organization (elastic modulus ~160 GPa). Figure 4B shows force-displacement curves done on mica and on agarose. The elastic deformation was determined by subtracting the trace obtained on mica from the compression curves obtained on biological samples (Fig. 4A). The force-displacement curve for mica is extremely steep (almost perpendicular to the z-axis), indicating a hard surface with little or no deformation occurring in contact with the cantilever. In contrast, nano-indentation (or compression) curves

obtained on a 2.5% agarose film had a much lower slope on the contact consistent with a soft material. The elastic (Young's) modulus, *E*, was estimated by fitting the contact region of the force-displacement curves using the Hertz model (Equation 1; solid line); the fits yielded an *E* of 25 ± 8 kPa, which is similar to published values (Loparic *et al.*, 2010; Stolz *et al.*, 2004).

We found that aorta collagen samples were able to undergo deformation within their elastic limits, returning to their original state when relaxed. The force-compression curves shows a nearly linear and reversible (unloading part of the force-displacement curve, data not shown) response to compression even after several repeated cycles, confirming the elastic property of the aortic collagen samples (Fig. 5A). AEEA treatment by the *in vivo* protocol leads to a clear increase in the slope of the force-compression curve.

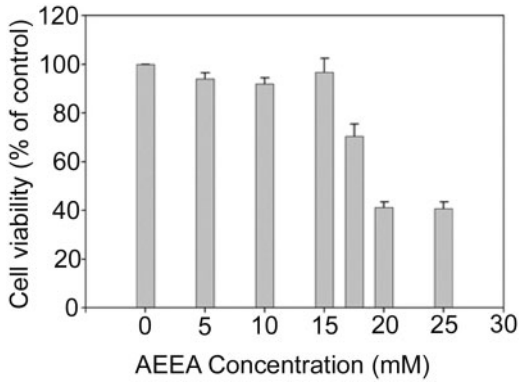

FIG. 2. The cytotoxic effects of AEEA to VSMCs: The standard MTT assay was performed to determine the cell viability. Cells were exposed to various concentrations of AEEA (0.0, 5.0, 10.0, 15.0, 17.5, 20.0, and 25.0 mM) for 24 h. Absorbance values read at 570 nm with a microplate reader were normalized to control wells. Five replicate wells were used for each assay. Values are the means SD of 3 separate experiments.

Figure 5B shows histograms and corresponding Gaussian distributions for stiffness measurements on untreated, AEEA treated; the respective contact slopes were 4.7 ± 1.2 and 9.7 ± 1.5 pN/nm. Hence, AEEA-treated aorta samples had a ~2-fold higher stiffness than those untreated. To quantify the tendency of aorta collagen samples to deform non-permanently (elastically) we determined the elastic Young's modulus. We measured an average elastic modulus of ~13 and 7 kPa for untreated and AEEA-treated aorta collagen, respectively. This suggests significant a stiffening of the 3D collagen nano-structure caused by AEEA.

Analysis of the Mechanical Properties of AEEA-Treated ECM Samples

Similar to the findings in aortic collagen, AEEA had a remarkable effect on the nano-mechanics of the ECM derived from rat aortic smooth muscle cells. Figure 6A shows compression curves obtained on samples treated with increasing concentrations of AEEA (0, 0.25, and 0.50 mM). The untreated ECM sample had a contact stiffness of ~10 pN/nm a value similar to 2.5% agarose (Fig. 6B). Treatment with 0.25 and 0.5 mM increased the contact stiffness to 14 and 38 pN/nm, respectively. This corresponds to an increase in Young's modulus from 25 kPa (untreated) to about 100 kPa, suggesting a stiffening of the ECM. The elastic modulus for the untreated ECM samples are in the range for those reported for cartilage ECM (~20–100 kPa; [Wilusz

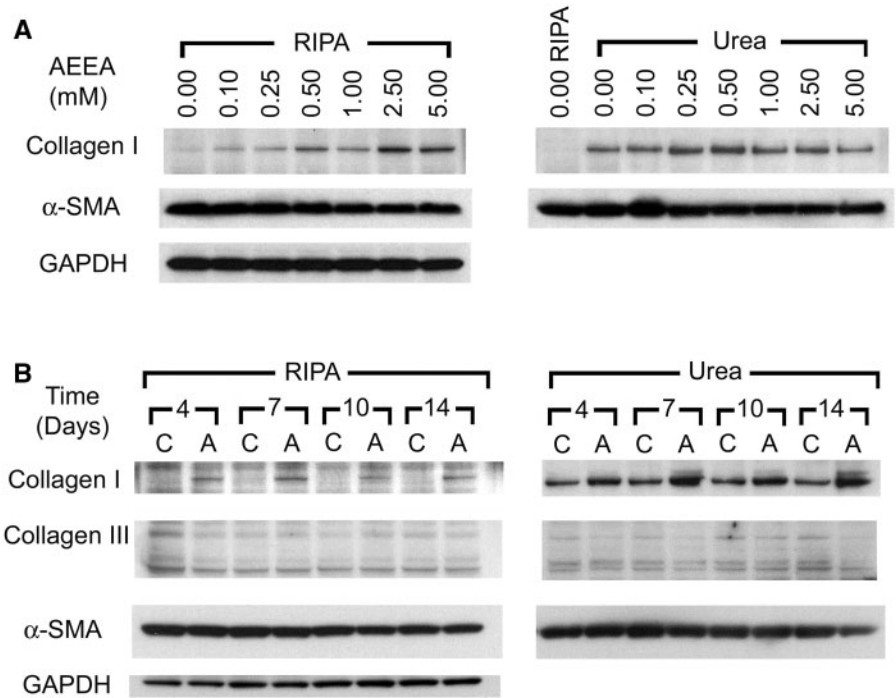

FIG. 3. Western blot studies of collagen type I and type III in cultures neonatal rat VSMCs treated with AEEA. **A**, VSMCs were treated with varying concentration of AEEA (0.00, 0.10, 0.25, 0.50, 1.00, 2.50, or 5.00 mM) for 10 days. The samples were serially extracted with RIPA buffer and then with urea extraction buffer, as described above. 20 μg of protein of each sample was separated with SDS-PAGE and transferred to PVDP membrane. The blots were detected with antibodies against collagen type I, and then re-probed with α-SMA and GAPDH, respectively. **B**, Time course studies of the effects of AEEA on the extractable collagen type I and type III proteins. The VSMCs were exposed to 0.50 mM AEEA for 4, 7, 10, or 14 days. The samples were serially extracted with RIPA buffer and then with urea extraction buffer. 20 μg of protein of each sample was separated with SDS-PAGE and transferred to PVDP membrane. The blots were detected with antibodies against collagen type I and III, and then re-probed with α-SMA and GAPDH, respectively. C = control; A = AEEA.

et al., 2012]) and cell-secreted ECMs (~27 kPa; [Engler *et al.*, 2007]).

Discussion

Aortic dissection is the most devastating thoracic aortic disease in humans. Dissection by definition is the disruption of the medial layer, or media of the vessel, and extension of blood along its wall. The media is composed predominantly of VSMC and their main intercellular protein products, collagen, and elastin (Boor *et al.*, 2006). Recognized for more than 250 years (Goldfinger *et al.*, 2014), arterial dissection can affect any large or medium-sized artery (including coronary arteries) but the commonest and most dramatic dissection begins in the thoracic aorta (DAA), with potential devastating effects on heart, lungs, brain, and upper extremities.

DAA is associated with hypertension of any cause (Golledge and Eagle, 2008) and has long been known to occur with high frequency in well-defined syndromes such as Marfan (Judge and Dietz, 2005), Ehlers-Danlos of the vascular form (Pyeritz, 2000), and Loeys-Dietz (Watanabe *et al.*, 2008). A familial form unassociated with a specific syndromic phenotype has also been described (Gleason, 2005; Pannu *et al.*, 2005; Tran-Fadulu *et al.*, 2006). The factors, either genetic or acquired, that underlie DAA in humans are thought to have in common some form of weakening of the interstitial matrix of the aortic media that allows for splitting of the medial layers (Golledge and Eagle, 2008). In the syndromic forms of DAA, emphasis has been placed on the Marfan syndrome, where 600 mutations of the gene for fibrillin-1 (*FBN1*) are now catalogued (Lee *et al.*, 1991; Pannu *et al.*, 2005). Fibrillin-1 is found at the periphery of the elastic fiber and is thought to serve as a scaffold for elastin formation (Nataatmadja *et al.*, 2003). Pathologic changes in the integrity and structure of the ECM of the aortic wall, including fragmentation of elastin, have long been known to occur in DAA, and altered expression of many ECM proteins has been shown (Nataatmadja *et al.*, 2003). Another means by what dysregulation in the intercellular matrix leading to DAA may occur is through the activation of TGF-β (Neptune *et al.*, 2003) or by mutations in *TGFBR1* and *TGFBR2* (Jamsheer *et al.*, 2009; Mizuguchi *et al.*, 2004; Pannu *et al.*, 2005). Defects in these genes have been described in the Loeys-Dietz syndrome (Loeys *et al.*, 2005, 2006).

Milewicz *et al.* (2008), in studies of a familial form of DAA, found genetic defects seemingly unrelated to fibrillin or TGFβ; these included defects predominantly in smooth-muscle-specific genes (*MYH11, ACTA2, and MLLK*). This finding draws attention to the importance of the role of smooth muscle cell function in preserving aortic structure that, when perturbed, may lead to changes in the characteristics of the intercellular matrix that result in aortic dissection.

Animal research plays a crucial role in our understanding of diseases and in the development of effective medical treatments. Although animal models of aortic aneurysm of the dilated type occurs in the abdominal aorta have been developed using genetic manipulation and chemical injury (Anidjar *et al.*, 1990;

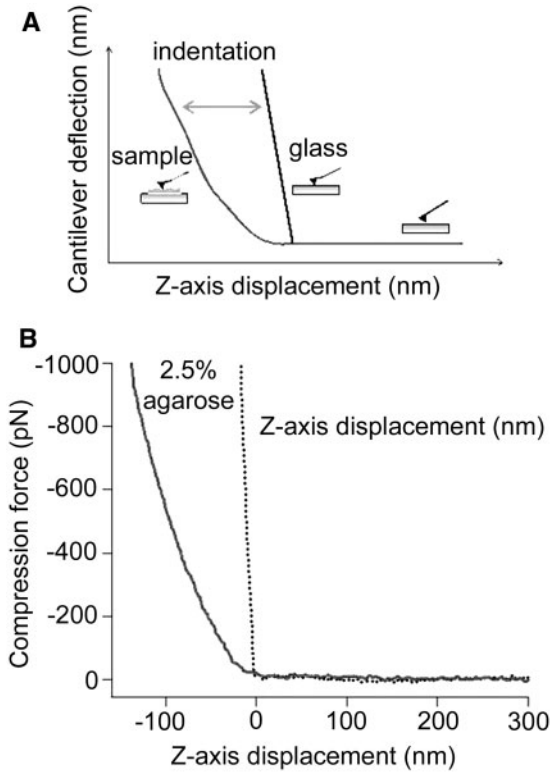

FIG. 4. Force versus displacement during compression cycles for a reference agarose film. **A**, Cartoon diagram of an idealized AFM compression experiment. The elastic deformation is calculated by subtracting a reference trace (F-x curve on mica) from the compression curve on collagen films. **B**, Elastic deformation curves obtained on mica and 2.5% agarose film. The agarose film serves as a calibration since its elastic modulus is well known (~0.02 MPa).

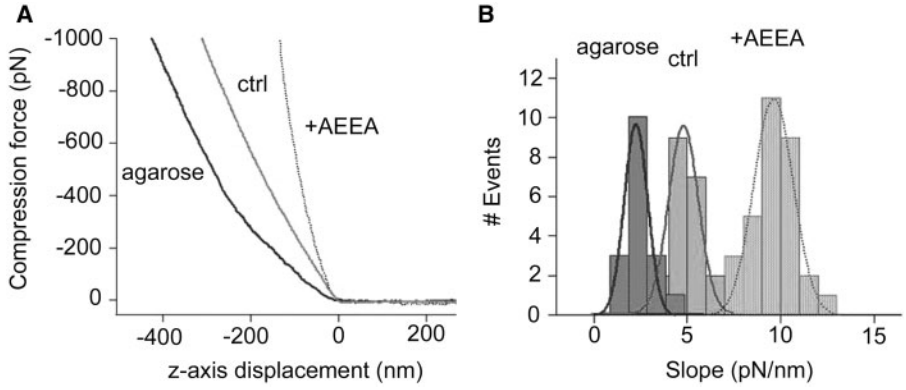

FIG. 5. Analysis of *in vivo* Aorta collagen samples using compression AFM. **A**, Force versus displacement during compression cycles for treated (+ AEEA) and untreated aorta samples (ctrl). The solid line corresponds to a force-displacement curve on 2.5% agarose film which serves as a reference point. **B**, Histograms showing the elasticity of different samples relative to agarose. The elasticity parameter was estimated by measuring the average slope of force-displacement curves. The lines correspond to Gaussian fits giving the following average slopes: 2.1 ± 0.9 pN/nm (2.5% agarose), 4.7 ± 1.2 pN/nm (untreated), and 9.7 ± 1.5 pN/nm (treated).

Daugherty and Cassis, 2004; Hynecek *et al.*, 2007; Sadek *et al.*, 2008; Tanaka *et al.*, 2009), models of DAA are few and nearly all use traumatic surgical procedures to induce dissections (Fujii *et al.*, 2000; Ikonomidis *et al.*, 2003; Terai *et al.*, 2005).

Most relevant to DAA, however, is the inactivation of the gene encoding collagen type III (Col3A1) in mutant mice created by Liu *et al.* (1997). In their study, homozygous ColL3A1 −/− mice had a survival of 5% at weaning and a phenotype that includes DAA morphologically identical to the developmental DAA described by our laboratory (Gong *et al.*, 2008). In further unpublished structural studies by electron microscopy in our *in vivo* model, however, we did not observe the swollen and otherwise abnormal collagen fibrils described by Liu *et al.* (1997). Col3A1 −/− mice die from ruptured DAA and also show intestinal enlargement and rupture, and defective wound healing. Liu *et al.* suggested that lack of type III collagen disrupts normal collagen fibrillogenesis and results in defective mature collagen type I fibrils in the media and adventitia of aorta, as well as in collagen of skin, lung, and heart. Collagen type III acts as a "procollagen" critically involved in fibrillogenesis and maturation of collagen type I, the main structural collagen in the adult. Interestingly, collagen type III is most abundant in vascular, and other, highly elastic tissues such as bowel, lung, and skin. Further support for a role of Col3A1 in defective aortic connective tissue is the demonstration of frameshift mutations in the Col3A1 gene in patients with Ehlers-Danlos Syndrome type IV, the dominantly inherited form of the disease characterized by large-joint hypermobility, thin and fragile skin, classic DAA, and bowel rupture (Schwarze *et al.*, 2001).

In this study, we again employ the environmental chemical-induced *in vivo* DAA model in which we previously addressed this developmental form of DAA that develops in offspring of rat dams given the industrial chemical AEEA (Gong *et al.*, 2006, 2008; Xu *et al.*, 2014). *In vitro* strategies, however, simplify the *in vivo* system under study, thus allowing investigators to focus on a small number of issues. In addition, the use of human cell lines helps to rule out possible species bias. Furthermore, *in vitro* systems are amenable to miniaturization, and may be developed for high-throughput screening methods to testing molecules for pharmacological or toxicological activity.

In this study, we utilized such an *in vitro* system of VSMCs to study the effects of AEEA on morphological, biochemical, and biophysical aberrations in vascular matrix associated with DAA. Complementary to our animal model, the *in vitro* studies proved highly reproducible with little generalized cell toxicity, combined with a very specific effect on the VSMCs associated with development of DAA.

Since cultured neonatal rat aortic smooth muscle cells are capable of depositing relatively large amounts of collagen and elastin in their ECM, they offer a perfect *in vitro* platform to investigate the mechanisms of AEEA-induced aberrations in ECM. Taking advantage of this *in vitro* strategy, we first observed striking morphological difference in ECM prepared from the AEEA-treated VSMCs when examined by routine optical microscope and the SEM.

Biochemical analysis is an important way to understand collagen aberrations in the vascular matrix that might be associated with DAA. Non-cross-linked collagens should be extractable, and collagen antibodies usually only detect the native collagen (eg, collagen type III antibody used in this study, ab7778). In our previous animal studies, we found a decreased content of collagen type I and III by native Western blot and by immunohistochemistry. We also localized structural proteins collagen and elastin via multi-photon fluorescence aorta and found a marked decrease in outer medial collagen type III, indicating developmental disruption. Therefore, in the present studies we first examined the non-cross-linked collagen type III in a native gel system (NuPAGE Novex 7% Tris-acetate protein gels ran with Tris-glycine native running buffer). We did not detect bands corresponding to collagen type III. Since the solubility of the non-cross-linked collagens is associated with the denaturing strength of the extracting solution, and RIPA buffer contains the ionic detergents SDS and sodium deoxycholate (and accordingly is more denaturing than NP-40 or Triton X-100 lysis buffer), we then extracted collagens with RIPA, followed by detection with SDS-PAGE. We consequently detected an increasing collagen type I, with greatest type I in samples extracted from AEEA-treated cells. The AEEA-associated increase was dose-dependent; though it was barely detectable in the cells not treated with AEEA (Figs. 3A and 3B). We could also detect collagen type III in most experiments (Fig. 3B).

Collagen type I is the most abundant ECM protein (Rossert *et al.*, 2000), comprising ~2/3 of the total collagen in human aortas (Murata *et al.*, 1986). Accordingly, collagen type III is clearly not as abundant as type I in VSMCs grown *in vitro* in these experiments, which may be in contrast to the situation in the fetal, developmental animal model. In addition, it has been shown that in maturation of a scar, abundant ECM is degraded and the immature type III collagen of the early wound matures into type I collagen (Niessen *et al.*, 1999; Slemp and Kirschner, 2006). This is consistent with our finding that collagen type III in control cells was higher at the earliest time point, eg, 4 days post-treatment (or 5 days post-seeding), and then dropped at later time points. Thus, the detailed role of collagen type III in cell culture systems such as we employed is yet to be investigated.

Our results showed that only a small fraction of non-cross-linked collagen was extractable in RIPA buffer (Fig. 3), even with the use of sufficient volumes of RIPA buffer to allow a protein concentration in the RIPA buffer of 2 μg/μl or lower. (At that concentration, in buffer used, most proteins should be solubilized). In order to better extract the non-cross-linked collagen, we further extracted pellets with urea (see section "Methods") by sequentially extracting after the RIPA extraction. Urea is a chaotropic denaturant which unravels the tertiary structure of proteins by destabilizing internal, non-covalent bond interactions (Pace, 1986). Proteins can be denatured by urea via several processes. One is the direct interaction of urea hydrogen bonds to polarized areas of charge, such as peptide groups. This affects intermolecular bonds and interactions, weakening the overall secondary and tertiary structure (Hua *et al.*, 2008). Once gradual protein unfolding occurs, water and urea can access more easily the hydrophobic inner core of the protein, speeding up the denaturation process (Bennion and Daggett, 2003; Hua *et al.*, 2008; Li *et al.*, 2012). We found that collagen type I was much more extractable in the urea buffer than in RIPA buffer, and this phenomenon was enhanced in the samples from the AEEA-treated cells (Fig. 3).

In aqueous buffers, the solubility of proteins depends on the distribution of exposed hydrophilic and hydrophobic amino acid residues. Proteins that have high hydrophilic amino acid content on the molecule's surface have higher solubility in an aqueous solvent (Pace *et al.*, 2004). In addition, detergents, salts, and pH of the buffer may affect the protein solubility. The isoelectric point value can affect the solubility of a protein molecule at a given pH. Such proteins have minimum solubility in water or salt solutions at the pH that corresponds to their isoelectric point and often precipitate out of solution. Solubility can also be strongly influenced by the type and the

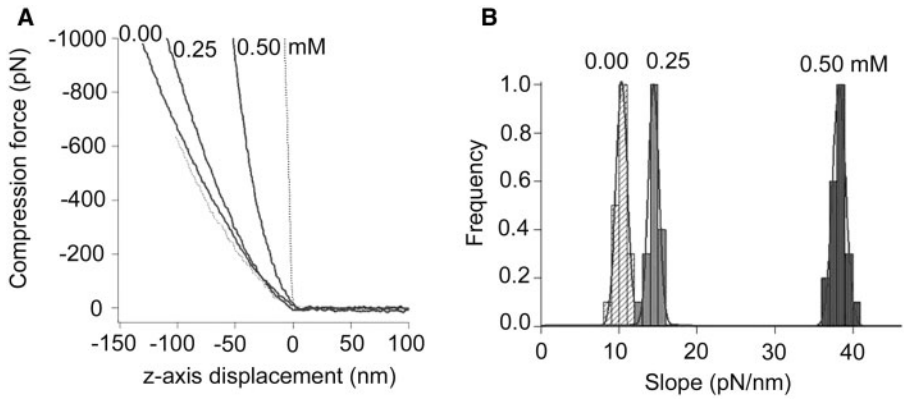

FIG. 6. Analysis of *in vitro* formed ECM samples using compression AFM. **A**, Force versus displacement during compression cycles obtained for samples with increasing concentrations of AEEA (0-0.50 mM) and untreated aorta samples (ctrl). The left dotted line corresponds to a force-displacement curve on 2.5% agarose film. The right dotted line corresponds to a force-displacement curve done on mica. **B**, Elasticity histograms of ECM samples treated with different concentrations of AEEA. The lines correspond to Gaussian fits giving the following average slopes: 9.85 ± 0.98 pN/nm (0.00 mM), 14.06 ± 1.2 pN/nm (0.25 mM), and 37.8 ± 1.1pN/nm (0.50 mM).

concentration of salts in the aqueous solution (Kumar and Venkatesu, 2014; Tome *et al.*, 2013). Moreover, the solubility of a protein may be regulated by protein post-translational modifications, eg, protein glycosylation (Cheng *et al.*, 2010; Helenius and Aebi, 2004; Ioannou *et al.*, 1998) and protein lipidation (Hang and Linder, 2011), and the interaction of a protein molecule to other molecules, such as protein (Baaden and Marrink, 2013) or lipid (Martfeld *et al.*, 2015). As a matter of fact, in our preliminary experiments, when we used the "SUMO-1-modified protein extraction buffer" (Adamson and Kenney, 2001) to extract our samples, like that of urea buffer, collagen type I was much more extractable in that buffer than in RIPA buffer. The "SUMO-1-modified protein extraction buffer" a 1:3 mixture of buffer I (5% SDS, 0.15 M Tris-HCl [pH 6.8], 30% glycerol) and buffer II (25 mM Tris-HCl [pH 8.3], 50 mM NaCl, 0.5% NP-40, 0.5% deoxycholate, 0.1% SDS, and protease inhibitors), which contains more SDS than that of RIPA buffer. The more detail mechanisms of why the non-cross-linked collagen was more extractable in the urea buffer and the "SUMO-1-modified protein extraction buffer" than in the RIPA buffer remain to be further investigated. However, the strategy of serial extraction provides a very useful way to further study these mechanisms.

In this study, while the collagen type I was much more extractable in the samples from the AEEA-treated VSMC, the sizes of the corresponding pellets became much smaller after urea buffer extraction (data not shown). This suggests that the impairment of collagen cross-linking in the ECM of the AEEA-treated cells might account for the change in the ECM underlying DAA. It also raises the possibility of inhibition of LOX, the collagen cross-linking enzyme, or activation of metalloproteases, which will be further investigated. Our *in vitro* studies further support the concept that abnormal collagen fibrillogenesis is the basic defect predisposing to dissection in this model. The increased extractable collagen type I observed suggests some critical change in the normal progression to mature collagen.

Elastin is also one of the important and major components of the ECM, particularly in the media of aorta, and its aberration may also be associated with DAA (Boor *et al.*, 2006). Whether AEEA causes an aberration in elastin yet remains to be more thoroughly studied, although our initial studies found no effect on total extractable aortic elastin, or fibrillins (Gong *et al.*, 2006).

Most importantly, this study demonstrated that AEEA has a significant effect on the mechanical properties of both aortic collagen (studied *in vivo*) and on ECM films produced *in vitro* by VSMCs, as measured by indentation AFM. The average elastic modulus for untreated aorta collagen was ~7 kPa, a value that is in the range to that of articular cartilage at the nanoscale level (Simha *et al.*, 2007; Stolz *et al.*, 2004), but 1000-fold lower than topoelastin films (Hu *et al.*, 2010). The elastic modulus for AEEA-treated aorta collagen was significantly higher (~12 kPa) indicating an important effect of AEEA on the internal mechanical nanostructure of the extracted collagen. Since the AFM-tip is smaller than the diameter of a collagen fiber, the reduction in the elastic modulus by AEEA treatment suggests an alteration in the aorta's fine structure, perhaps due to an alteration of the 3D organization of collagen fibers. Similarly, AEEA had a clear effect on the rat aortic SMCs-derived ECM; AEEA treatment increased the Young's modulus from 25 to about 100 kPa, suggesting a decrease of elasticity in the collagen-elastin network. The more detail mechanisms of how such a decrease in elasticity is associated to the weakening of the interstitial matrix of the aortic media that allows for splitting of the medial layers need to be further studied.

A further important consideration in such combined *in vivo* and *in vitro* studies such as this is the dose utilized. In our earlier development of this developmental animal model of DAA, we found a clear direct dose-response relationship for incidence and degree of DAA in offspring of rat dams treated with AEEA by gavage in the range 10.0-150.0 mg/kg. In the *in vitro* portions of this study, the range of exposure to cells over a continuous period of 10 days was 0.10-0.50 mM. Since the *in vivo* absorption and tissue distribution of AEEA in the rat is not well known, it is difficult to precisely compare these dosage methods. Nevertheless, it seems reasonable that the higher mg/kg doses in the dams would reach mM levels in the tissues of the fetus. It is also important to note that in our original descriptions of the animal model, no overt toxicity was evident in AEEA-treated dams, and that includes the finding that dams did not develop DAA or any other signs of toxicity (Gong *et al.*, 2006; Xu *et al.*, 2014).

To conclude, in 2 experimental systems, both *in vivo* and *in vitro*, the biophysical changes in aortic collagen associated with developing DAA were found by AFM to be essentially identical, ie, the collagen is harder, or more brittle, and less elastic. This may well reflect the essential change that results in tearing of the vascular wall along the planes of the media that are essentially constructed by the VSMC. In biochemical studies, our data implicate a remarkable aberration in collagen I that is consistent with some defect in cross linkage of this critical structural interstitial protein. These findings, which we have

associated with the dramatic morphologic lesion of DAA, point out that a subtle effect on the VSMC may have huge detrimental effects on the integrity of the vessel wall.

FUNDING

NIH Grants R21-ES013038 and R21-ES022821 from the National Institute of Environmental Health and Safety support this work. The kind donation of AEEA by Dow Chemical Company and BASF, 67056 Ludwigshafen, Germany, is gratefully acknowledged. Portions of original studies upon which this work was based were funded by BASF through the Ethyleneamines Product Stewardship Discussion Group, Ludwigshafen, Germany.

ACKNOWLEDGMENTS

We thank Dr. Vsevolod L. Popov for his expert assistance with the scanning electron microscopic studies. We also thank the Ida and Cecil M. Green Endowment at the University of Texas Medical Branch for their generous support.

REFERENCES

Achterberg, V. F., Buscemi, L., Diekmann, H., Smith-Clerc, J., Schwengler, H., Meister, J. J., Wenck, H., Gallinat, S., and Hinz, B. (2014). The nano-scale mechanical properties of the extracellular matrix regulate dermal fibroblast function. *J. Invest. Dermatol.* **134**, 1862–1672.

Adamson, A. L., and Kenney, S. (2001). Epstein-barr virus immediate-early protein BZLF1 is SUMO-1 modified and disrupts promyelocytic leukemia bodies. *J. Virol.* **75**, 2388–2399.

Alcaraz, C., De Diego, M., Pastor, M. J., and Escribano, J. M. (1990). Comparison of a radioimmunoprecipitation assay to immunoblotting and ELISA for detection of antibody to African swine fever virus. *J. Vet. Diagn. Invest.* **2**, 191–1966.

Anidjar, S., Salzmann, J. L., Gentric, D., Lagneau, P., Camilleri, J. P., and Michel, J. B. (1990). Elastase-induced experimental aneurysms in rats. *Circulation* **82**, 973–981.

Arteaga-Solis, E., Gayraud, B., and Ramirez, F. (2000). Elastic and collagenous networks in vascular diseases. *Cell Struct. Funct.* **25**, 69–72.

Baaden, M., and Marrink, S. J. (2013). Coarse-grain modelling of protein-protein interactions. *Curr. Opin. Struct. Biol.* **23**, 878–886.

Bennion, B. J., and Daggett, V. (2003). The molecular basis for the chemical denaturation of proteins by urea. *Proc. Natl Acad. Sci. U. S. A.* **100**, 5142–5147.

Bertram, C., and Hass, R. (2009). Cellular senescence of human mammary epithelial cells (HMEC) is associated with an altered MMP-7/HB-EGF signaling and increased formation of elastin-like structures. *Mech. Ageing Dev.* **130**, 657–669.

Boor, P. J., Yang, Y., and Gong, B. (2006). Role of the media in vascular injury: atherosclerosis and dissection. *Toxicol. Pathol.* **34**, 33–38.

Bourget, J. M., Gauvin, R., Larouche, D., Lavoie, A., Labbe, R., Auger, F. A., and Germain, L. (2012). Human fibroblast-derived ECM as a scaffold for vascular tissue engineering. *Biomaterials* **33**, 9205–9213.

Bullard, B., Linke, W. A., and Leonard, K. (2002). Varieties of elastic protein in invertebrate muscles. *J. Muscle Res. Cell. Motil.* **23**, 435–447.

Chandrakasan, G., Torchia, D. A., and Piez, K. A. (1976). Preparation of intact monomeric collagen from rat tail tendon and skin and the structure of the nonhelical ends in solution. *J. Biol. Chem.* **251**, 6062–6067.

Cheng, S., Edwards, S. A., Jiang, Y., and Grater, F. (2010). Glycosylation enhances peptide hydrophobic collapse by impairing solvation. *Chemphyschem* **11**, 2367–2374.

Criado, F. J. (2011). Aortic dissection: a 250-year perspective. *Tex. Heart Inst. J.* **38**, 694–700.

Daugherty, A., and Cassis, L. A. (2004). Mouse models of abdominal aortic aneurysms. *Arterioscler. Thromb. Vasc. Biol.* **24**, 429–434.

Davidson, J. M., LuValle, P. A., Zoia, O., Quaglino, D., Jr., and Giro, M. (1997). Ascorbate differentially regulates elastin and collagen biosynthesis in vascular smooth muscle cells and skin fibroblasts by pretranslational mechanisms. *J. Biol. Chem.* **272**, 345–352.

Elefteriades, J. A. (2008). Thoracic aortic aneurysm: reading the enemy's playbook. *Yale J. Biol. Med.* **81**, 175–186.

Engler, A. J., Rehfeldt, F., Sen, S., and Discher, D. E. (2007). Microtissue elasticity: measurements by atomic force microscopy and its influence on cell differentiation. *Methods Cell Biol.* **83**, 521–545.

Florin, E.-L., Rief, M., Lehmann, H., Ludwig, M., Dornmair, C., Moy V. T., and Gaub, H. E. (1995). Sensing specific molecular interactions with the atomic force microscope. *Biosens. Bioelectron.* **10**, 895–901.

Foti, C., Bonamonte, D., Mascolo, G., Tiravanti, G., Rigano, L., and Angelini, G. (2001). Aminoethylethanolamine: a new allergen in cosmetics?. *Contact Dermatitis* **45**, 129–133.

Frey, M. T., Engler, A., Discher, D. E., Lee, J., and Wang, Y. L. (2007). Microscopic methods for measuring the elasticity of gel substrates for cell culture: microspheres, microindenters, and atomic force microscopy. *Methods Cell Biol.* **83**, 47–65.

Fujii, H., Tanigawa, N., Okuda, Y., Komemushi, A., Sawada, S., and Imamura, H. (2000). Creation of aortic dissection model in swine. *Jpn. Circ. J.* **64**, 736–737.

Gleason, T. G. (2005). Heritable disorders predisposing to aortic dissection. *Semin. Thoracic Cardiovasc. Surg.* **17**, 274–281.

Goh, C. L. (1985). Occupational dermatitis from soldering flux among workers in the electronics industry. *Contact Dermatitis* **13**, 85–90.

Goldfinger, J. Z., Halperin, J. L., Marin, M. L., Stewart, A. S., Eagle, K. A., and Fuster, V. (2014). Thoracic aortic aneurysm and dissection. *J. Am. Coll. Cardiol.* **64**, 1725–1739.

Golledge, J., and Eagle, K. A. (2008). Acute aortic dissection. *Lancet* **372**, 55–66.

Gong, B., Trent, M. B., Srivastava, D., and Boor, P. J. (2006). Chemical-induced, nonlethal, developmental model of dissecting aortic aneurysm. *Birth Defects Res. A Clin. Mol. Teratol.* **76**, 29–38.

Gong, B., Sun, J., Vargas, G., Chang, Q., Xu, Y., Srivastava, D., and Boor, P. J. (2008). Nonlinear imaging study of extracellular matrix in chemical-induced, developmental dissecting aortic aneurysm: evidence for defective collagen type III. *Birth Defects Res. A Clin. Mol. Teratol.* **82**, 16–24.

Graham, R. C., Jr., and Karnovsky, M. J. (1966). The early stages of absorption of injected horseradish peroxidase in the proximal tubules of mouse kidney: ultrastructural cytochemistry by a new technique. *J. Histochem. Cytochem.* **14**, 291–302.

Hang, H. C., and Linder, M. E. (2011). Exploring protein lipidation with chemical biology. *Chem. Rev.* **111**, 6341–6358.

He, N. G., Awasthi, S., Singhal, S. S., Trent, M. B., and Boor, P. J. (1998). The role of glutathione S-transferases as a defense

against reactive electrophiles in the blood vessel wall. *Toxicol. Appl. Pharmacol.* **152**, 83–89.

Helenius, A., and Aebi, M. (2004). Roles of N-linked glycans in the endoplasmic reticulum. *Annu. Rev. Biochem.* **73**, 1019–1049.

Hu, X., Wang, X., Rnjak, J., Weiss, A. S., and Kaplan, D. L. (2010). Biomaterials derived from silk-tropoelastin protein systems. *Biomaterials* **31**, 8121–8131.

Hua, L., Zhou, R., Thirumalai, D., and Berne, B. J. (2008). Urea denaturation by stronger dispersion interactions with proteins than water implies a 2-stage unfolding. *Proc. Natl Acad. Sci. U. S. Am.* **105**, 16928–16933.

Hynecek, R. L., DeRubertis, B. G., Trocciola, S. M., Zhang, H., Prince, M. R., Ennis, T. L., Kent, K. C., and Faries, P. L. (2007). The creation of an infrarenal aneurysm within the native abdominal aorta of swine. *Surgery* **142**, 143–149.

Ikonomidis, J. S., Gibson, W. C., Gardner, J., Sweterlitsch, S., Thompson, R. P., Mukherjee, R., and Spinale, F. G. (2003). A murine model of thoracic aortic aneurysms. *J. Surg. Res.* **115**, 157–163.

Ioannou, Y. A., Zeidner, K. M., Grace, M. E., and Desnick, R. J. (1998). Human alpha-galactosidase A: glycosylation site 3 is essential for enzyme solubility. *Biochem. J.* **332**, 789–797.

Jamsheer, A., Henggeler, C., Wierzba, J., Loeys, B., De Paepe, A., Stheneur, C., Badziag, N., Matuszewska, K., Matyas, G., and Latos-Bielenska, A. (2009). A new sporadic case of early-onset Loeys-Dietz syndrome due to the recurrent mutation p.R528C in the TGFBR2 gene substantiates interindividual clinical variability. *J. Appl. Genet.* **50**, 405–410.

Judge, D. P., and Dietz, H. C. (2005). Marfan's syndrome. *Lancet* **366**, 1965–1976.

Kumar, A., and Venkatesu, P. (2014). Does the stability of proteins in ionic liquids obey the Hofmeister series? *Int. J. Biol. Macromol.* **63**, 244–253.

Langford, S. D., Trent, M. B., and Boor, P. J. (2002). Semicarbazide-sensitive amine oxidase and extracellular matrix deposition by smooth-muscle cells. *Cardiovasc. Toxicol.* **2**, 141–150.

Lee, B., Godfrey, M., Vitale, E., Hori, H., Mattei, M. G., Sarfarazi, M., Tsipouras, P., Ramirez, F., and Hollister, D. W. (1991). Linkage of Marfan syndrome and a phenotypically related disorder to two different fibrillin genes. *Nature* **352**, 330–334.

Li, W., Zhou, R., and Mu, Y. (2012). Salting effects on protein components in aqueous NaCl and urea solutions: toward understanding of urea-induced protein denaturation. *J. Phys. Chem. B* **116**, 1446–1451.

Lin, D. C., Dimitriadis, E. K., and Horkay, F. (2007). Robust strategies for automated AFM force curve analysis—I. Non-adhesive indentation of soft, inhomogeneous materials. *J. Biomech. Eng.* **129**, 430–440.

Liu, X., Wu, H., Byrne, M., Krane, S., and Jaenisch, R. (1997). Type III collagen is crucial for collagen I fibrillogenesis and for normal cardiovascular development. *Proc. Natl Acad. Sci. U. S. A.* **94**, 1852–1856.

Loeys, B. L., Chen, J., Neptune, E. R., Judge, D. P., Podowski, M., Holm, T., Meyers, J., Leitch, C. C., Katsanis, N., Sharifi, N., *et al.* (2005). A syndrome of altered cardiovascular, craniofacial, neurocognitive and skeletal development caused by mutations in TGFBR1 or TGFBR2. *Nat. Genet.* **37**, 275–281.

Loeys, B. L., Schwarze, U., Holm, T., Callewaert, B. L., Thomas, G. H., Pannu, H., De Backer, J. F., Oswald, G. L., Symoens, S., Manouvrier, S., *et al.* (2006). Aneurysm syndromes caused by mutations in the TGF-beta receptor. *N. Engl. J. Med.* **355**, 788–798.

Loparic, M., Wirz, D., Daniels, A. U., Raiteri, R., Vanlandingham, M. R., Guex, G., Martin, I., Aebi, U., and Stolz, M. (2010). Micro- and nanomechanical analysis of articular cartilage by indentation-type atomic force microscopy: validation with a gel-microfiber composite. *Biophys. J.* **98**, 2731–2740.

Martfeld, A. N., Rajagopalan, V., Greathouse, D. V., and Koeppe, R. E., 2nd (2015). Dynamic regulation of lipid-protein interactions. *Biochimica et Biophysica Acta* **1848**, 1849–1859.

Milewicz, D. M., Guo, D. C., Tran-Fadulu, V., Lafont, A. L., Papke, C. L., Inamoto, S., Kwartler, C. S., and Pannu, H. (2008). Genetic basis of thoracic aortic aneurysms and dissections: focus on smooth muscle cell contractile dysfunction. *Annu. Rev. Genomics Hum. Genet.* **9**, 283–302.

Miller, E., Garcia, T., Hultgren, S., and Oberhauser, A. F. (2006). The mechanical properties of *E. coli* type 1 pili measured by atomic force microscopy techniques. *Biophys. J.* **91**, 3848–3856.

Mizuguchi, T., Collod-Beroud, G., Akiyama, T., Abifadel, M., Harada, N., Morisaki, T., Allard, D., Varret, M., Claustres, M., Morisaki, H., *et al.* (2004). Heterozygous TGFBR2 mutations in Marfan syndrome. *Nat. Genet.* **36**, 855–860.

Moore, N. P., Tornesi, B., Yano, B. L., Nitschke, K. D., and Carney, E. W. (2012). Developmental sensitivity to the induction of great vessel malformations by N-(2-aminoethyl)ethanolamine. *Birth Defects Res. B Dev. Reprod. Toxicol.* **95**, 116–122.

Murata, K., Motayama, T., and Kotake, C. (1986). Collagen types in various layers of the human aorta and their changes with the atherosclerotic process. *Atherosclerosis* **60**, 251–262.

Nakamura, H. (1988). Electron microscopic study of the prenatal development of the thoracic aorta in the rat. *Am. J. Anat.* **181**, 406–418.

Nataatmadja, M., West, M., West, J., Summers, K., Walker, P., Nagata, M., and Watanabe, T. (2003). Abnormal extracellular matrix protein transport associated with increased apoptosis of vascular smooth muscle cells in marfan syndrome and bicuspid aortic valve thoracic aortic aneurysm. *Circulation* **108**(Suppl 1), II329–II334.

Neptune, E. R., Frischmeyer, P. A., Arking, D. E., Myers, L., Bunton, T. E., Gayraud, B., Ramirez, F., Sakai, L. Y., and Dietz, H. C. (2003). Dysregulation of TGF-beta activation contributes to pathogenesis in Marfan syndrome. *Nat. Genet.* **33**, 407–411.

Ngoka, L. C. (2008). Sample prep for proteomics of breast cancer: proteomics and gene ontology reveal dramatic differences in protein solubilization preferences of radioimmunoprecipitation assay and urea lysis buffers. *Proteome Sci.* **6**, 30.

Niessen, F. B., Spauwen, P. H., Schalkwijk, J., and Kon, M. (1999). On the nature of hypertrophic scars and keloids: a review. *Plast. Reconstr. Surg.* **104**, 1435–1458.

Oakes, B. W., Batty, A. C., Handley, C. J., and Sandberg, L. B. (1982). The synthesis of elastin, collagen, and glycosaminoglycans by high density primary cultures of neonatal rat aortic smooth muscle. An ultrastructural and biochemical study. *Eur. J. Cell Biol.* **27**, 34–46.

Oberhauser, A. F., Marszalek, P. E., Erickson, H. P., and Fernandez, J. M. (1998). The molecular elasticity of the extracellular matrix protein tenascin. *Nature* **393**, 181–185.

Pace, C. N. (1986). Determination and analysis of urea and guanidine hydrochloride denaturation curves. *Methods Enzymol.* **131**, 266–280.

Pace, C. N., Trevino, S., Prabhakaran, E., and Scholtz, J. M. (2004). Protein structure, stability and solubility in water and other solvents. *Philos. Trans. R. Soc. Lond. B Biol. Sci.* **359**, 1225–1234; discussion 1234–1235.

Pannu, H., Tran-Fadulu, V., and Milewicz, D. M. (2005). Genetic basis of thoracic aortic aneurysms and aortic dissections. *Am. J. Med. Genet. Semin. Med. Genet.* **139C**, 10–16.

Pepys, J., and Pickering, C. A. (1972). Asthma due to inhaled chemical fumes—amino-ethyl ethanolamine in aluminium soldering flux. *Clin. Allergy* **2**, 197–204.

Pyeritz, R. E. (2000). Ehlers-Danlos syndrome. *N. Engl. J. Med.* **342**, 730–732.

Rabbi, M., and Marszalek, P. E. (2007). Construction of a single-axis molecular puller for measuring polysaccharide and protein mechanics by atomic force microscopy. *CSH Protoc* **2007**, pdb prot4899.

Rossert, J., Terraz, C., and Dupont, S. (2000). Regulation of type I collagen genes expression. *Nephrol. Dial. Transplant.* **15**(Suppl 6), 66–68.

Sadek, M., Hynecek, R. L., Goldenberg, S., Kent, K. C., Marin, M. L., and Faries, P. L. (2008). Gene expression analysis of a porcine native abdominal aortic aneurysm model. *Surgery* **144**, 252–258.

Schwarze, U., Schievink, W. I., Petty, E., Jaff, M. R., Babovic-Vuksanovic, D., Cherry, K. J., Pepin, M., and Byers, P. H. (2001). Haploinsufficiency for one COL3A1 allele of type III procollagen results in a phenotype similar to the vascular form of Ehlers-Danlos syndrome, Ehlers-Danlos syndrome type IV. *Am. J. Hum. Genet.* **69**, 989–1001.

Simha, N. K., Jin, H., Hall, M. L., Chiravarambath, S., and Lewis, J. L. (2007). Effect of indenter size on elastic modulus of cartilage measured by indentation. *J. Biomech. Eng.* **129**, 767–775.

Slemp, A. E., and Kirschner, R. E. (2006). Keloids and scars: a review of keloids and scars, their pathogenesis, risk factors, and management. *Curr. Opin. Pediatr.* **18**, 396–402.

Sterling, G. M. (1967). Asthma due to aluminium soldering flux. *Thorax* **22**, 533–537.

Stolz, M., Raiteri, R., Daniels, A. U., VanLandingham, M. R., Baschong, W., and Aebi, U. (2004). Dynamic elastic modulus of porcine articular cartilage determined at two different levels of tissue organization by indentation-type atomic force microscopy. *Biophys. J.* **86**, 3269–3283.

Tanaka, A., Hasegawa, T., Chen, Z., Okita, Y., and Okada, K. (2009). A novel rat model of abdominal aortic aneurysm using a combination of intraluminal elastase infusion and extraluminal calcium chloride exposure. *J. Vasc. Surg.* **50**, 1423–1432.

Terai, H., Tamura, N., Yuasa, S., Nakamura, T., Shimizu, Y., and Komeda, M. (2005). An experimental model of Stanford type B aortic dissection. *J. Vasc. Intervent. Radiol. JVIR* **16**, 515–519.

Tome, L. I., Pinho, S. P., Jorge, M., Gomes, J. R., and Coutinho, J. A. (2013). Salting-in with a salting-out agent: explaining the cation specific effects on the aqueous solubility of amino acids. *J. Phys. Chem. B* **117**, 6116–6128.

Tran-Fadulu, V., Chen, J. H., Lemuth, D., Neichoy, B. T., Yuan, J., Gomes, N., Sparks, E., Kramer, L. A., Guo, D., Pannu, H., *et al.* (2006). Familial thoracic aortic aneurysms and dissections: 3 families with early-onset ascending and descending aortic dissections in women. *Am. J. Med. Genet. A* **140**, 1196–1202.

Watanabe, Y., Sakai, H., Nishimura, A., Miyake, N., Saitsu, H., Mizuguchi, T., and Matsumoto, N. (2008). Paternal somatic mosaicism of a TGFBR2 mutation transmitting to an affected son with Loeys-Dietz syndrome. *Am. J. Med. Genet. A* **146A**, 3070–3074.

Wilusz, R. E., Defrate, L. E., and Guilak, F. (2012). A biomechanical role for perlecan in the pericellular matrix of articular cartilage. *Matrix Biol.* **31**, 320–327.

Xu, Y., Treumann, S., Rossbacher, R., Schneider, S., and Boor, P. J. (2014). Dissecting aortic aneurysm induced by N-(2-aminoethyl) ethanolamine in rat: role of defective collagen during development. *Birth Defects Res. A Clin. Mol. Teratol.* **100**, 924–933.

Yang, Y., Yang, Y., Trent, M. B., He, N., Lick, S. D., Zimniak, P., Awasthi, Y. C., and Boor, P. J. (2004). Glutathione-S-transferase A4–4 modulates oxidative stress in endothelium: possible role in human atherosclerosis. *Atherosclerosis* **173**, 211–221.